Biochemical and Biophysical Research Communications 441 (2013) 904–910

Contents lists available at ScienceDirect

Biochemical and Biophysical Research Communications

journal homepage: www.elsevier.com/locate/ybbrc

Autocrine galectin-1 promotes collective cell migration of squamous cell carcinoma cells through up-regulation of distinct integrins

Andra Rizqiawan, Kei Tobiume *, Gaku Okui, Kazuhiro Yamamoto, Hideo Shigeishi, Shigehiro Ono, Hiroshi Shimasue, Masaaki Takechi, Koichiro Higashikawa, Nobuyuki Kamata

Department of Oral and Maxillofacial Surgery, Graduate School and Institute of Biomedical and Health Sciences, Hiroshima University, Hiroshima 734-8553, Japan

ARTICLE INFO

Article history:
Received 18 October 2013
Available online 7 November 2013

Keywords:
EMT
Snail
Galectin-1
Collective cell migration

ABSTRACT

We found that high galectin-1 (Gal-1) mRNA levels were associated with invasive squamous cell carcinoma (SCC) cells that expressed Snail, an epithelial-to-mesenchymal transition (EMT) regulator. Both Gal-1 overexpression and soluble Gal-1 treatment accelerated invasion and collective cell migration, along with activation of cdc42 and Rac. Soluble Gal-1 activated c-Jun N-terminal kinase to increase expression levels of integrins α2 and β5, which were essential for Gal-1 dependent collective cell migration and invasiveness. Soluble Gal-1 also increased the incidence of EMT in Snail-expressing SCC cells; these were a minor population with an EMT phenotype under growing conditions. Our findings indicate that soluble Gal-1 promotes invasiveness through enhancing collective cell migration and increasing the incidence of EMT.

1. Introduction

Epithelial-to-mesenchymal transition (EMT) is a process by which a cancer cell becomes invasive. The process is typically characterized by loss of the cell–cell adhesion molecule E-cadherin, and acquisition of the mesenchymal protein vimentin [1,2]. Snail is a zinc finger transcription factor, and a master regulator of EMT that triggers the process through direct repression of E-cadherin expression [1,2]. Previous microarray analyses using oral squamous cell carcinoma (SCC) cells indicate that 63 genes, including Gal-1, are involved in Snail-induced EMT [3].

Gal-1 is a member of the β-galactoside-binding lectin family of proteins. These are expressed at various levels in many tissues under normal and pathological conditions. It has been reported that increased Gal-1 expression in SCC tissues is associated with prognosis. Gal-1 localizes to the nucleus and cytoplasm, and is present in the extracellular matrix. Regardless of whether the signal peptide is absent from its primary polypeptide sequence, Gal-1 exists as a non-covalent homodimer in its secreted form. This binds to the galactoside group in a glycosylated protein *via* a carbohydrate recognition domain [4–6].

During this study, we elucidated a novel mechanism through which autocrine Gal-1 induces cell migration and invasion by up-regulating the expression of integrins α2 and β5 through c-Jun N-terminal kinase (JNK) signaling pathways.

2. Materials and methods

2.1. Cell culture and reagents

The human vulval SCC cell line A431, and the human oral SCC cell lines OM-1, HOC719-PE, HOC719-NE, and HOC 313 were maintained as described previously [3,7]. HEK293FT cells were purchased from Invitrogen (CA, USA). All cell lines were cultured in Dulbecco's modified Eagle's medium (Sigma–Aldrich, MO, USA), supplemented with 10% fetal bovine serum (Biowest, Tokyo, Japan) and 1% penicillin streptomycin (Sigma–Aldrich) at 37 °C/5% CO_2. The JNK inhibitor SP600125 and the nuclear factor-kappa B (NF-kB) inhibitor ammonium pyrrolidinedithiocarbamate (APDC) were purchased from Sigma–Aldrich. Human recombinant galectin-1 (#450-39) was obtained from Peprotech (NJ, USA). Primary antibodies included those directed against Galectin-1 (sc-28248; Santa Cruz Biotech, TE, USA), V5 (Invitrogen), E-cadherin (#3195; Cell Signaling Technology, MA, USA), integrin α2 (CD49b) (#611016; BD Biosciences, CA, USA), integrin β5 (#4708; Cell Signaling Technology), phospho-JNK (#4668; Cell Signaling Technology), phospho-c-Jun (#9261; Cell Signaling Technology) and glyceraldehyde 3-phosphate dehydrogenase (GAPDH; MAB374; Millipore, MA, USA). We purchased horseradish peroxidase (HrP)-conjugated anti-rabbit IgG and HrP-conjugated anti-mouse IgG from GE Healthcare Bio-Sciences. Neutralizing antibodies against integrin

* Corresponding author. Address: Institute of Biomedical and Health Sciences, Hiroshima University, 1-2-3 Kasumi, Minami-ku, Hiroshima 734-8553, Japan. Fax: +81 82 257 5671.
E-mail address: tobi5651@hiroshima-u.ac.jp (K. Tobiume).

0006-291X/$ - see front matter © 2013 Elsevier Inc. All rights reserved.
http://dx.doi.org/10.1016/j.bbrc.2013.10.152

α2 (MAB1950), integrin β1 (MAB1987) and integrin αV (MAB1980) were purchased from Millipore.

2.2. Reverse-transcription polymerase chain reaction (PCR) assays

Total RNA was isolated using an RNeasy kit (Qiagen, Venlo, Netherlands). First strand cDNA synthesis was conducted with cDNA synthesis kits (Toyobo, Osaka, Japan). Aliquots of the first strand cDNA library were subjected to PCR using Go tag Green Master Mix (Promega, WI, USA) when amplicons were to be subjected to agarose gel electrophoresis. For real-time detection, we used Thunderbird™ SYBR® qPCR Mix (Toyobo) in quantitative PCR (qPCR) assays. Gene-specific primer pairs are presented in Supplementary Table 1. The qPCR data were analyzed using a CFX connect Real-Time PCR Detection System (Bio-Rad, CA, USA). Relative comparison of samples with a calibrator was determined according to the Thunderbird™ SYBR® qPCR Mix (Toyobo) user manual.

2.3. Plasmids

The Galectin-1 (NM_002305.3) open reading frame was amplified from an OM-1 cDNA library using LA Taq with a GC buffer kit (Takara, Shiga, Japan) and cloned into a pCR8 Gateway entry plasmid (Invitrogen) using a pCR8/GW/TOPO TA cloning kit (Invitrogen). The entry vector was converted into pLenti 6.2/V5-DEST (Invitrogen) using an LR recombinase II kit (Invitrogen). This resulted in a V5-tagged Gal-1-expressing pLenti plasmid. The V5-tagged Snail-expressing pLenti plasmid has been previously described [8].

2.4. Recombinant virus production and infection

The ViraPower™ Letiviral Packaging Mix was purchased from Invitrogen. Host HEK293FT cells were co-transfected with pLenti plasmid and ViraPower™ using FuGENE6 (Promega), according to the manufacturer's protocol. After 48 h, the virus-containing supernatant supplemented with 8 μg/ml polybrene (Sigma) was used to infect target cells. Uninfected cells were removed by the addition of 10 μg/ml blasticidin (Invitrogen) during culture.

2.5. Immunoblotting

Cells harvested in phosphate-buffered saline (PBS) were precipitated and suspended in lysis buffer from a Mammalian Cell Lysis Kit (Sigma–Aldrich). For secreted proteins, growth medium was replaced with serum-free medium, and cells were incubated for a further 3 h. The conditioned medium was incubated with 4 volumes of acetone at −20 °C for 1 h. After centrifugation (15,000g, 10 min, 4 °C) the protein precipitate was dissolved in lysis buffer from the Mammalian Cell Lysis Kit. Total protein concentration was determined using a BCA protein assay kit (Pierce, IL, USA). Protein samples (20 μg) were denatured and reduced in sample buffer (ATTO) separated using 4–20% gradient sodium dodecyl sulfate polyacrylamide gel electrophoresis and transferred to Immobilon-P (Millipore) membranes. The membranes were incubated (12 h, 4 °C) with the appropriate primary antibody diluted in Tris-buffered saline supplemented with Triton-X100 and 5% (w/v) bovine serum albumin (BSA). The immunoblot was labeled with the appropriate HrP-conjugated secondary antibody and signals visualized with an ECL Advance Western Blotting Detection Kit (GE Healthcare Bio-Sciences). Acquired images were analyzed using a LAS 4000 mini (GE Healthcare Bio-Sciences).

2.6. Pull-down assays

Cells were harvested using an Active GTPase Pull-Down and Detection kit (Pierce) according to the manufacturer's instruction. Briefly, a cell extract was applied to each affinity column for the GTP-bound form of Rho, Rac or cdc42. The bound fraction was eluted and recovered in sample buffer. Cell extracts and bound fractions were subjected to immunoblotting with anti-Rho, anti-Rac and anti-cdc42 antibodies, which were supplied in the kit.

2.7. Wound healing assays

Confluent monolayers of cells were prepared in culture plates. Wounds were prepared by scraping each plate with a sterile 200-μl pipette tip. Initial wound size and closing distance was evaluated using phase-contrast microscope images at various time points using a BZ-9000 microscope (Keyence, Osaka, Japan).

2.8. In vitro three-dimensional culture

Immortalized fibroblast GT1 cells were suspended in type I collagen (Koken, Tokyo, Japan) containing growth medium, then poured into 12-well culture plates [9]. Subsequently, 1×10^6 SCC cells in 1 ml of growth medium were seeded onto the collagen gel. After 1 week in culture, a small shrunken gel disc was placed onto a reversed nylon mesh strainer well (BD Biosciences) to maintain the air–liquid interface culture for a further week. Each gel was fixed with Mildform (Wako, Osaka, Japan) and embedded in paraffin. Thinly sliced sections were stained with hematoxylin and eosin (HE; Wako) and analyzed.

2.9. Invasion assays

Invasiveness was assessed using Biocoat-Matrigel invasion chambers (BD Biosciences) according to the manufacturer's instructions. Briefly, 2.5×10^5 cells were seeded into each upper chamber and cultured for 24 h. The upper chamber was fixed by soaking in 4% paraformaldehyde in PBS. After removing cells from the topside of the Matrigel-coated membrane, cells invading the other side of the membrane were stained with HE and counted with the aid of a microscope.

2.10. RNA interference (RNAi)

Small interfering RNAs (siRNAs) for integrin β5 and control siRNAs were obtained from Sigma Aldrich. Target-specific siRNA duplexes were 5′-CUA UGU CUG CGG CCU GUG UTT-3′ (sense) and 5′-ACA CAG GCC GCA GAC AUA GTT-3′ (antisense). We transfected 2.5×10^5 cells were with 100 pmol of double-stranded (ds)RNA using RNAi Max (Invitrogen) according to the manufacturer's guidelines. The knock-down efficiency was determined 48 h later by immunoblotting with an anti-integrin β5 antibody (data not shown). Wound healing assays were started at 24 h post-transfection once cells were confluent.

2.11. Fluorescent cell imaging

Cells were seeded in 24-well EZ view glass-bottom plates (Iwaki, Shizuoka, Japan), fixed with 4% paraformaldehyde in PBS for 15 min, and permeabilized with 0.2% Triton X-100 in PBS for 30 min. The permeabilization step was omitted for cell surface staining analysis. Cells were incubated for 8 h with a primary antibody incubated in PBS containing 5% (w/v) BSA, and subsequently incubated for 1 h with Alexa Fluor® 568- or Alexa Fluor® 488-conjugated secondary antibodies (Invitrogen). To visualize F-actin, cells were incubated with Alexa Fluor® 488 Phalloidin (Invitrogen) diluted in PBS for

30 min, following fixation and permeabilization. Cells were mounted in Vectashield anti-fade medium containing 4′,6-diamidino-2-phenylindole (DAPI; Vector Laboratories, CA, USA). Fluorescence images were acquired with a BZ-9000 microscope (Keyence).

2.12. Statistical analysis

Results were expressed as the mean ± SD. Group comparisons were evaluated using Tukey's test. Two groups were compared using Student's *t*-test. A *P*-value less than 0.05 was considered statistically significant. Analyses were conducted using Mathematica (Wolfram Research, IL, USA).

3. Results

3.1. Gal-1 upregulation is concomitant with Snail-induced EMT

Since microarray analysis retrieved Gal-1 as one of highly upregulated gene in Snail-dependent EMT [3], we confirmed that SCC cells with an EMT phenotype expressed higher levels of Gal-1 than non-EMT SCC cells at the mRNA and protein levels (Fig. 1A and B). We also confirmed up-regulation of Gal-1 via exogenous Snail expression in these cells (Fig. 1C). Because Gal-1 promoter possesses a NF-kB binding motif [10] and Snail-expressing SCC cells showed higher NF-kB activity [11], we tested whether Snail-expressing SCC cells required NF-kB to up-regulate Gal-1. The NF-kB inhibitor APDC suppressed Gal-1 up-regulation in Snail-expressing SCC cells (Fig. 1D), indicating that Snail indirectly up-regulates Gal-1 *via* NF-kB. To evaluate the effects of elevated Gal-1 expression on non-EMT SCC cells, V5-tagged Gal-1 was stably expressed (Fig. 1E). This did not result in reduced levels of E-cadherin, nor induction of vimentin, which are both hallmarks of EMT (Fig. 1E and F).

3.2. Gal-1 induces collective cell migration and invasiveness of SCC cells

Although we did not observe a typical EMT phenotype in exogenous Gal-1-expressing SCC cells (Fig. 1E and F), we found that these cells exhibited accelerated wound healing (Fig. 1G and Supplementary Fig. S1A). The cells also exhibited greater levels of invasiveness than parental SCC cells (Fig. 1H). The consequence of Gal-1-dependent invasiveness was further evaluated using *in vitro* three-dimensional cultures [9]. Whereas parental SCC cells showed a multilayered epithelial structure, Gal-1 expressing SCC cells lacked this structure (Fig. 2A). Gal-1-expressing SCC cells retained homophilic cell adhesion but invaded the stroma (Fig. 2A). Gal-1-expressing SCC cells markedly enhanced filopodia formation during collective cell migration, whereas parental SCC cells exhibited cortical staining of F-actin (Fig. 2B). The amounts of GTP-bound cdc42/Rac were consistently increased in Gal-1-expressing SCC cells (Fig. 2C), whereas GTP-bound RhoA was undetectable (Fig. 2C).

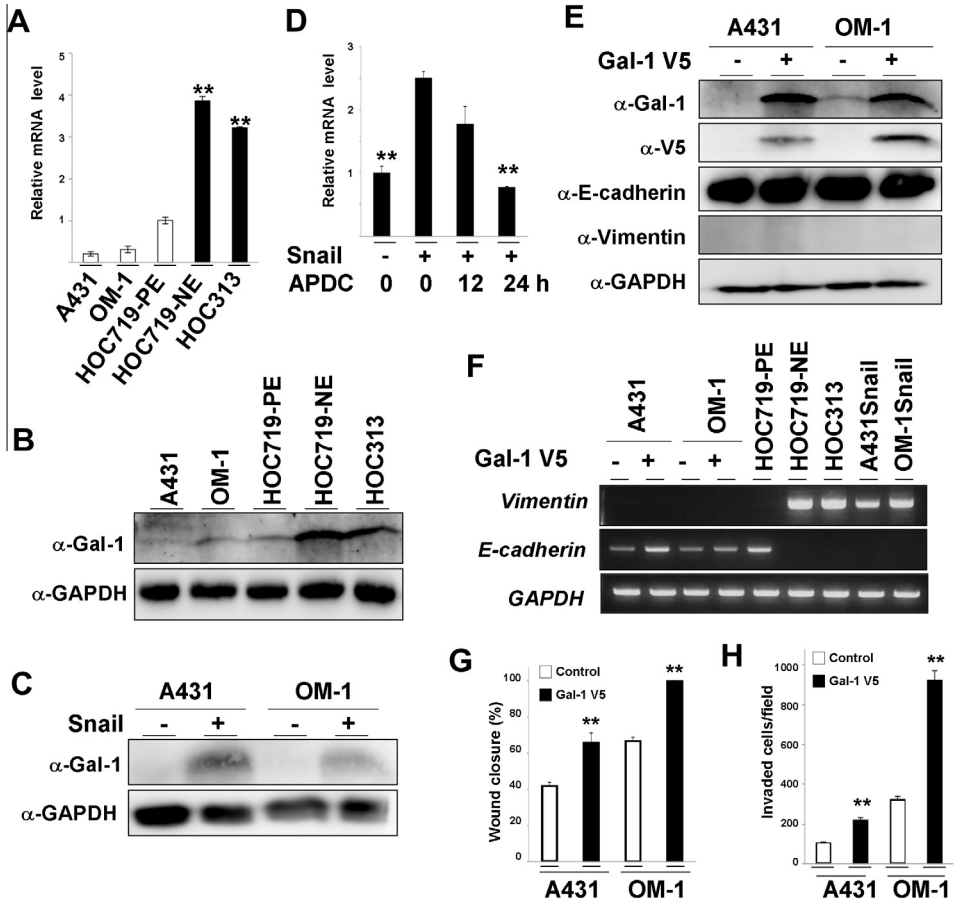

Fig. 1. Gal-1 expression confers collective cell migration and invasiveness. (A) Expression levels of Gal-1 mRNA in indicated SCC cell lines. Values are presented as mean ± SD for three experiments (**$p < 0.05$: significantly large, Tukey's test). (B) Expression levels of the Gal-1 protein in SCC cells from (A). (C) Expression levels of Gal-1 in indicated SCC cells with (+) or without (−) exogenous Snail expression. (D) Relative comparison of Gal-1 mRNA with an NFkB inhibitor (APDC) (**$p < 0.05$: significantly small to other two groups, Tukey's test). (E) Immunoblotting analysis of total cell lysates from SCC cell lines with (+) or without (−) V5-tagged Gal-1 (Gal-1 V5). (F) Assessment of EMT using mRNA expression profiles with Vimentin and E-cadherin. (G) Wound healing assays on confluent monolayer of cells expressing Gal-1 (Gal-1 V5). Data are expressed as % of wound closure at 24 h (mean ± SD) from six different microscopic fields of view (**$p < 0.05$: significant increase, Student's *t*-test). (H) Biocoat-Matrigel invasion assay with Gal-1 expression (Gal-1 V5). The number of invaded cells is expressed as mean ± SD from 6 different fields of view (**$p < 0.05$: significant increase, Student's *t*-test).

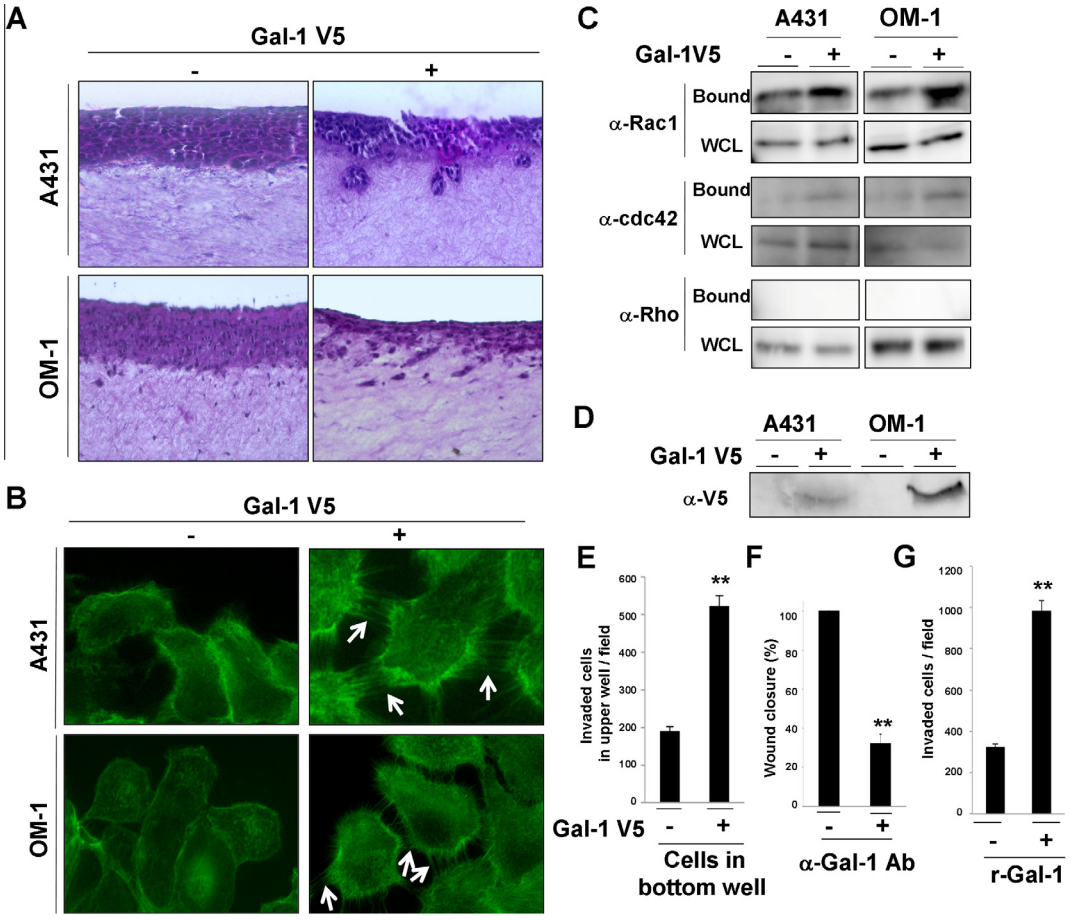

Fig. 2. Soluble Gal-1 promotes filopodia formation, collective cell migration and invasiveness. (A) Histological analysis of SCC cells in three-dimensional cultures. (B) SCC cells were fixed at 24 h in the wound healing assays. Arrowheads indicate filopodia formation. (C) Evaluation of GTP-bound small G proteins. Cell extracts from indicated cells were subjected to affinity columns for purification of GTP-bound small G proteins (Rac, cdc42 and Rho). Input cell extract (WCL) and bound fraction (Bound) were subject to immunoblotting with indicated antibodies. (D) Immunoblot of conditioned medium from SCC cells with (+) or without (−) Gal-1 expression (Gal-1 V5). (E) OM-1 cells were co-cultured with (+) or without (−) Gal-1 expression (Gal-1 V5) in the Biocoat-Matrigel invasion assays. Invaded OM-1 cell numbers from the upper wells are presented as the mean ± SD from six different fields (**$p < 0.05$: significant increase, Student's *t*-test). (F) Wound healing assay for Gal-1-expressing OM-1 cells with (+) or without (−) anti-Gal-1 antibodies (α-Gal-1 Ab) in the culture medium. Wound healing was expressed as % of wound closure at 24 h to initial wound distance (mean ± SD) as determined from six different fields of view (**$p < 0.05$: significant decrease, Student's *t*-test). (G) Biocoat-Matrigel invasion assay using OM-1 cells with (+) or without (−) recombinant Gal-1 (r-Gal-1). Invaded cell numbers are presented as the mean ± SD from six different fields of view (**$p < 0.05$: significant increase, Student's *t*-test).

Since Gal-1 is known to function as both an intracellular protein and an extracellular soluble protein [4–6], we assessed whether secreted Gal-1 affected phenotypes. We confirmed that the culture supernatant of Gal-1-expressing SCC cells contained secreted soluble Gal-1 (Fig. 2D). To test the biological activity of conditioned medium, Gal-1-expressing SCC cells and parental SCC cells were co-cultured in Biocoat-Matrigel invasion assays. When Gal-1 expressing cells were seeded in the bottom well, more SCC cells on the upper well invaded (Fig. 2E). Wound healing of confluent Gal-1-expressing cells was markedly delayed in the presence of an anti-Gal-1 antibody (Fig. 2F and Supplementary Fig. S1B), indicating soluble autocrine Gal-1 conferred phenotypes. The enhancement of invasiveness (Fig. 2G), wound healing (Supplementary Fig. S1C), and actin-remodeling (Supplementary Fig. S1D) were also achieved using a recombinant version of the protein. This confirmed the contributions of soluble Gal-1.

3.3. Autocrine Gal-1 upregulates integrins α2 and β5 to enhance collective cell migration and invasiveness

As the process for collective cell migration involves various integrins [12–14], we assessed integrin expression profiles. Gal-1-expressing cells exhibited marked upregulation of integrins α2 and β5 at the mRNA and protein level (Fig. 3A and B). Recombinant Gal-1 also increased the expression levels of integrins α2 and β5 in SCC cells in a time-dependent manner (Fig. 3C). The contribution of autocrine Gal-1 to the expression of these integrins was further confirmed by blocking secreted Gal-1 in Gal-1-expressing SCC cells. The addition of an anti-Gal-1 antibody to cell cultures reduced integrin α2 (Fig. 3D) and integrin β5 (Supplementary Fig. S1E) levels. Recombinant Gal-1 increased integrin α2 mRNA levels within 3 h (Fig. 3E), when the surface integrin α2 accumulated clearly at the base of the forming filopodium (Fig. 3F). To assess the contribution of integrin α2 to Gal-1-dependent collective cell migration, Gal-1-expressing SCC cells were subject to wound healing assays with neutralizing anti-integrin α2 antibodies. We also tested the neutralizing anti-integrin β1 antibody as a block to the functional integrin complex comprising the α2 subunit (i.e., integrin α2β1) [12]. Neutralization of integrins α2 and β1 specifically delayed wound healing of Gal-1-expressing SCC cells (Fig. 3G and Supplementary Fig. S1F). Neutralization of integrins α2 and β1 also prevented recombinant Gal-1-mediated invasiveness (data not shown). Because of an unavailability of neutralizing antibody against integrin β5, we tested the possible contribution of an integrin complex comprising integrin β5 (i.e., integrin αVβ5)[12]. Neutralization of integrin αV and specific siRNA-mediated silencing of integrin β5 suppressed the wound healing abilities of Gal-1-expressing SCC cells (Fig. 3G, Supplementary Fig. S1F and G).

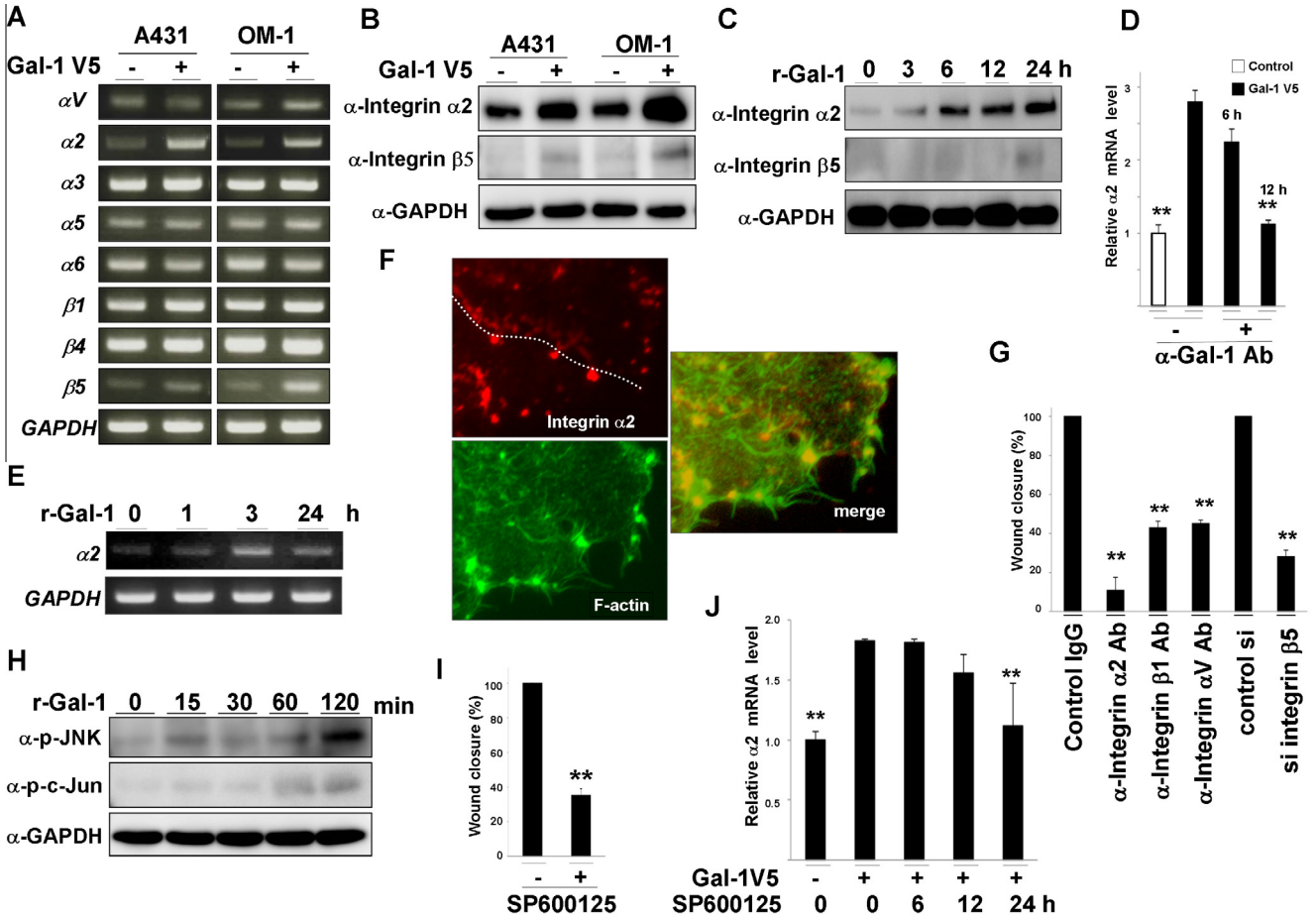

Fig. 3. Gal-1 up-regulates distinct integrin subunits to promote invasiveness. (A) mRNA expression levels for various epithelial integrins in SCC cells with (+) or without (−) Gal-1 expression (Gal-1 V5). (B) Immunoblot of SCC cells from (A). (C) Immunoblot of recombinant Gal-1 (r-Gal-1)-treated OM-1 with anti-integrin α2 and anti-Integrin β5. (D) Cells were incubated with an anti-Gal-1 antibody (α-Gal-1 Ab) as indicated. Relative expression levels for integrin α2 are presented as the mean ± SD from three independent experiments (**$p < 0.05$: significantly small to other two groups, Tukey's test). (E) Increased integrin α2 mRNA levels in cells from (C). (F) Immunocytochemistry analysis and F actin visualization of cells from (C) at 6 h. Immunostaining with an anti-integrin α2 antibody was conducted without permeabilization, after which F-actin was labeled with Alexa Fluor® 488-conjugated phalloidin with permeabilization. The dotted lines in the upper panel indicate the boundary of two cells. (G) Wound healing assay for Gal-1-expressing OM-1 cells with indicated antibodies or siRNAs. Wound healing is expressed as % of wound closure at 24 h (mean ± SD) from six different fields of view (**$p < 0.05$: significant decrease, Student's *t*-test). (H) JNK activation in OM-1 cells incubated with 8 μg/ml recombinant Gal-1 (r-Gal-1). Cell extracts were prepared at various time points and subjected to immunoblotting with indicated antibodies. (I) Wound healing assay for Gal-1-expressing OM-1 cells. Cells were treated with (+) or without (−) 40 mM SP600125 for 24 h. Wound healing is expressed as % of wound closure at 24 h (mean ± SD) from six different fields of view (**$p < 0.05$: significantly small to another, Student's *t*-test). (H) Relative expression levels for integrin α2 mRNAs in OM1 cells that underwent various treatments. Data are expressed as mean ± SD from three independent experiments (**$p < 0.05$: significantly small to other groups, Tukey's test).

3.4. Gal-1 activates JNK to induce distinct integrins for collective cell migration

To determine the pathway for Gal-1-dependent integrin expression, we assessed several protein kinases using immunoblotting; however, Gal-1 had no effects on these protein kinases (data not shown). We managed to identify JNK, where Gal-1-dependent activation was further confirmed by increased phosphorylation of its substrate, c-Jun (Fig. 3H). Incubation with SP600125, a specific inhibitor of JNK, during the wound healing assay clearly attenuated wound healing of Gal-1-expressing SCC cells (Fig. 3I and Supplementary Fig. S1E). SP600125 consistently suppressed mRNA expression levels of integrins α2 (Fig. 3J) and β5 (data not shown) in Gal-1-expressing SCC cells.

3.5. Gal-1 increases EMT incidence in Snail-expressing SCC cells

Although exogenous Snail expression in OM-1 cells increases EMT incidence, fewer than 30% of Snail-expressing OM-1 cells underwent EMT under growing conditions [8]. When these cells became confluent, cells with the EMT phenotype were less obvious, indicating EMT *via* Snail in OM-1 was reversible [8]. To determine the possible contribution of soluble Gal-1 to Snail-dependent EMT, Snail-expressing OM-1 cells were incubated with recombinant Gal-1 protein. Confluent Snail-expressing OM-1 cells, where the EMT population was lost [8], exhibited collective cell migration after wounding rather than a scattering of single cells into the wound area (Fig. 4A). The addition of recombinant Gal-1 accelerated not only collective cell migration of Snail-expressing SCC cells but increased the incidence of EMT in the wound area (Fig. 4A). E-cadherin and vimentin mRNA levels confirmed a higher susceptibility to EMT in response to wounding for the confluent monolayer (Fig. 4B). The incidence of EMT in Snail-expressing OM-1 cells under growing conditions was also significantly elevated to 42% with recombinant Gal-1 (Fig. 4C and D). However, neither anti-Gal-1 nor anti-integrin α2 antibodies displayed reduced EMT incidence for Snail-expressing OM-1 cells under growing conditions (Fig. 4D).

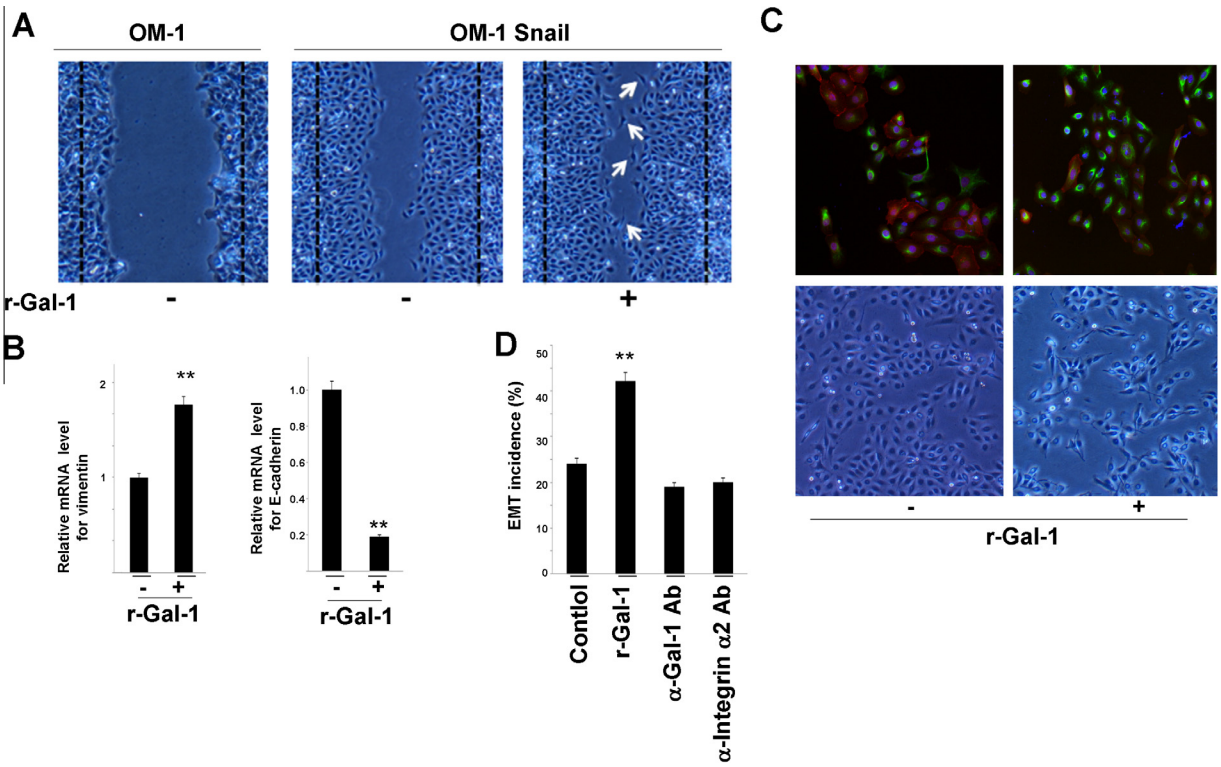

Fig. 4. Soluble Gal-1 increases the incidence of EMT for Snail-expressing SCC cells. (A) Confluent monolayers were treated with (+) or without (−) 8 μg/ml recombinant Gal-1 (r-Gal-1) and wounded. Exogenous Snail expression (OM-1Snail) was conducted. Phase-contrast images show wound healing at 7 h. Dotted lines indicate initial wound area; arrow heads indicate a cell with EMT morphology. (B) Relative mRNA expression levels for E-cadherin and vimentin at 7 h in the wound healing assay with (+) or without (−) recombinant Gal-1 (r-Gal-1). Multiple wounds were applied to each confluent monolayer. Data are expressed as the mean ± SD from three independent experiments (**$p < 0.05$: significantly changed, Student's *t*-test). (C) Immunocytochemistry and phase-contrast images of growing Snail-expressing OM-1 cells. Cells were inoculated when they were 70% confluent and treated with (+) or without (−) 8 μg/ml recombinant Gal-1(r-Gal-1) for 24 h. Cells were stained with anti-E-cadherin and anti-Vimentin antibodies simultaneously and visualized with Alexa Fluor® 568 (red)- and Alexa Fluor® 488 (green)-conjugated antibodies, respectively. Nuclei were visualized with DAPI (blue). (D) EMT incidence in variously treated Snail-expressing OM-1 cells. Incidence of EMT was expressed as a % of EMT versus total cells (mean ± SD) from three independent experiments (**$p < 0.05$: significantly large to other three groups, Tukey's test). (For interpretation of the references to color in this figure legend, the reader is referred to the web version of this article.)

4. Discussion

We revealed that soluble Gal-1 up-regulated integrin α2 and β5 expression *via* the JNK pathway; subsequently, the collective cell migration of SCC cells was increased. Several groups have previously reported that some galectins recognize target cells *via* galactoside-conjugated integrin subunits [15]. However, our results regarding Gal-1-dependent biological effects indicated integrins were effector molecules that promote collective cell migration. Although the role of galactoside-conjugated proteins and/or lipid molecules on the cell surface of soluble Gal-1 remains unclear, JNK was activated by a soluble Gal-1-dependent signaling pathway, and lead the specific up-regulation of integrins. Collective cell migration during the wound healing process in skin was recently shown to require integrin α2 for massive filopodia formation [13,14]. Our findings demonstrated that autocrine Gal-1 promoted a similar process in SCC cells, although it was possible that JNK activated cell motility *via* other pathways resulting in up-regulation of integrin expression. If the local concentration of soluble Gal-1 was increased, homophilic SCC cells would be able to form invading nests *via* collective cell migration. We previously reported that several cytokines promoted the incidence of EMT in Snail-expressing SCC cells *via* AKT-dependent collective cell migration [8]. In contrast, Gal-1 activated the JNK pathway but not the AKT pathway (data not shown) to increase collective cell migration. These findings indicate that that several signaling pathways could increase the incidence of EMT in Snail-expressing SCC cells. This might explain why blocking Gal-1 or integrin α2 alone failed to suppress the basal incidence of EMT in Snail-expressing OM-1 cells. A recent histochemical analysis of oral SCC specimens clearly showed that the quantity of Gal-1 protein was greater in stromal cells than in SCC nests, which comprised homophilic tumor cells in early SCC lesions [16,17]. Our result that soluble Gal-1 resulted in collective cell migration indicates that production of Gal-1 from cancer stromal cells also promotes invasive nest formation. In contrast, the SCC cells showed high Gal-1 protein expression levels in progressive SCC lesions, where tumor cells lost their homophilic attachments [16,17]. If tumor cells were predisposed to EMT *via* Snail, an elevated level of autocrine Gal-1 might result in progressive diffuse lesion development with a high incidence of EMT.

Appendix A. Supplementary data

Supplementary data associated with this article can be found, in the online version, at http://dx.doi.org/10.1016/j.bbrc.2013.10.152.

References

[1] R. Kalluri, R.A. Weinberg, The basic of epithelial mesenchymal transition, J. Clin. Invest. 119 (2009) 1420–1428.

[2] M.A. Nieto, The snail superfamily of zinc finger transcription factor, Nat. Rev. Mol. Cell Biol. 3 (2002) 155–166.

[3] K. Higashikawa, S. Yoneda, M. Taki, H. Shigeishi, S. Ono, K. Tobiume, N. Kamata, Gene expression profiling to identify gene associated with high-invasiveness

in human squamous cell carcinoma with epithelial-to-mesencyhmal transition, Cancer Lett. 264 (2008) 256–264.
[4] I. Camby, M.L. Mercier, F. Lefranc, R. Kiss, Galectin-1: a small protein with major functions, Glycobiology 16 (2006) 137–157.
[5] F. Liu, G.A. Rabinovich, Galectins as modulator of tumour progression, Nat. Rev. 5 (2005) 29–41.
[6] F.T. Liu, G.A. Rabinovich, Galectins : regulators of acute and chronic inflammation, Ann. N. Y. Acad. Sci. 1183 (2010) 158–182.
[7] M. Taki, N. Kamata, K. Yokoyama, R. Fujimoto, S. Tsutsumi, M. Nagayama, Down-regulation of Wnt-4 and up-regulation of Wnt-5a expression by epithelial-mesenchymal transition in human squamous carcinoma cells, Cancer Sci. 7 (2003) 593–597.
[8] G. Okui, K. Tobiume, A. Rizqiawan, K. Yamamoto, H. Shigeishi, S. Ono, K. Higashikawa, N. Kamata, AKT primes Snail-induced EMT concomitantly with the collective migration of squamous cells, J. Cell. Biochem. (2013), http://dx.doi.org/10.1002/jcb.24545.
[9] K. Higashikawa, S. Yoneda, M. Taki, H. Shigeishi, K. Tobiume, N. Kamata, Snail induced down-regulation of ΔNp63α acquires invasive phenotype of human squamous cell carcinoma, Cancer Res. 67 (2007) 9207–9213.
[10] M.A. Toscano, L. Campgna, L.L. Molinero, J.P. Cerliani, D.O. Croci, J.M. Ilarregui, M.B. Fuertes, I.M. Nojek, J.P. Fededa, N.W. Zwirner, M.A. Costas, G.A. Rabinovich, Nuclear factor (NF)-κB controls expression of the immunoregulatory glycan-binding protein galectin-1, Mol. Immunol. 48 (2011) 1940–1949.
[11] F. Tanaka, A. Rizqiawan, K. Higashikawa, K. Tobiume, G. Okui, H. Shigeishi, S. Ono, H. Shimasue, N. Kamata, Snail promotes Cyr61 secretion to prime collective cell migration and form invasive tumor nest in squamous cell carcinoma, Cancer Lett. 329 (2) (2013) 243–252.
[12] Y. Takada, X. Ye, S. Simon, The Integrins, Genome Biol. 8 (2007) 215.
[13] P. Friedl, D. Gilour, Collective cell migration in morphogenesis, regeneration and cancer, Nat. Rev. Mol. Cell Biol. 10 (2009) 445–457.
[14] O. Ilina, P. Friedl, Mechanisms of collective cell migration at a glance, J. Cell Sci. 122 (2009) 3203–3208.
[15] M.A. Romaniuk, D.O. Croci, M.J. Lapponi, M.V. Tribulatti, S. Negrotto, F. Poirier, O. Campetella, G.A. Rabinovich, M. Schattner, Binding of galectin-1 to Ilb3 integrin triggers "outside-in" signals, stimulates platelet activation, and control primary hemostasis, FASEB J. (2012) 197511–197541.
[16] L. Zhong, K. Wei, X. Yang, H. Pan, D. Ye, L. Wang, Z. Zhang, Overexpression of galecetin-1 is negatively correlated with pathological grade in oral squamous cell carcinoma, J. Cancer Res. Clin. Oncol. 136 (2010) 1527–1535.
[17] W.F. Chiang, S.Y. Liu, L.Y. Fang, C.N. Lin, M.H. Wu, Y.C. Chen, Y.L. Chen, Y.T. Jin, Overexpression of galectin-1 at the tumor invasion front is associated with poor prognosis in early-stage oral squamous cell carcinoma, Oral Oncol. 44 (2007) 325–334.